

# Comparison of One-Dimensional and Volume Distributed Feedback in Microwave Vacuum Electronic Devices

S. N. Sytova\*

*Research Institute for Nuclear Problem, Belarusian State University,  
11 Bobruiskaya Str., 220030 Minsk, BELARUS*

(Received 30 November, 2012)

Simulation and comparison of one-dimensional and volume distributed feedback in microwave vacuum electronic devices were accomplished. The first situation corresponds to conditions of backward-wave tube. The second one is the generation of radiation by relativistic electron beam in photonic (electromagnetic) crystal in conditions of Volume Free Electron Laser (VFEL). Obtained numerical results demonstrate that there exists an optimal set of parameters for effective generation and it is not located in one-dimensional geometry.

**PACS numbers:** 41.60.Cr; 35Q60, 35F20, 65M06

**Keywords:** Volume Free Electron Laser, mathematical modelling, chaos

## 1. Introduction

The main aim of this paper is simulation of processes of radiation generation by relativistic electron beam in photonic (electromagnetic) crystal in conditions of Volume Free Electron Laser (VFEL). In VFEL when relativistic electron beam passing through photonic crystals in conditions of dynamical diffraction, quasi-Cherenkov parametric radiation appears [1], [2]. According to special law valid only for VFEL [1]–[5], under diffraction in degeneration points the threshold current of electron beam obeys the following estimation:

$$j_{start} \sim \frac{1}{(kL)^{3+2s}} \quad (1)$$

where  $s$  is a number of surplus waves appearing in the system because of diffraction.  $k$  is a wave number,  $L$  is a length of photonic crystal.

This law is valid for all wavelength ranges and substantially differs from its analogues for electronic devices such as travelling wave tubes (TWT), backward-wave tubes (BWT), free electron lasers (FEL) etc. For any other electronic vacuum device except for VFEL there isn't dependence of threshold condition on the number of surplus waves appearing in the system due to

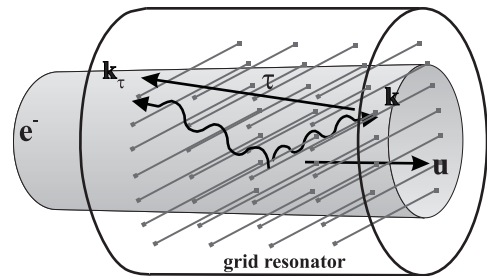


FIG. 1: VFEL with grid resonator.

diffraction. For BWT, TWT, FEL as well as for different types of cyclotron masers, Cherenkov plasma oscillators and other devices the beam threshold current is with power 3 [6]–[8] instead of  $3 + 2s$  in denominator like in estimation (1) given above.

(1) means the noticeable reduction of electron beam current density necessary for achievement the generation threshold in comparison with other devices and actual feasibility of setup miniaturization.

In vacuum electronic devices an interaction of moving forward electrons in a bunch with a stream of energy of electromagnetic waves occurs usually under one-dimensional distributed feedback where electrons and electromagnetic waves spread along one straight line: in one direction (TWT) or in opposite directions (BWT). The

\*E-mail: sytova@inp.bs.u.by

main feature of VFEL is non-one-dimensional volume distributed feedback (VDFB) where all electromagnetic waves and vector of electron velocity are situated angularly one to another.

Theory and experiments of VFEL were developed in [1]–[5], [10]–[12]. Recent experiments are carried out on INP VFEL setup with so-called grid resonator [12]. Such resonator is a tube with a system of metallic treads strained inside resonator with special periods (see Fig.1). In [10] it is demonstrated that such resonator is an example of photonic crystal [13], [14]. [15] was devoted to investigation of Cerenkov radiation arising in photonic crystals. In [16] proposed photonic Free Electron Lasers (pFEL) are based on Cerenkov radiation in photonic crystals. It is obvious that VFEL is a version of pFEL with additional special features like (1) and others [4].

In [17]–[22] VFEL was investigated numerically and examined as dynamical chaotic system. All main VFEL physical laws as well as generation thresholds for INP VFEL experimental setups were obtained numerically. It was demonstrated that there exists an optimal set of VFEL parameters for effective generation. A gallery of different chaotic regimes for VFEL laser intensity with corresponding phase space portraits, bifurcation diagrams, attractors and Poincare maps was proposed. It was denoted the necessity of taking into account the dispersion of electromagnetic waves on photonic crystal for microwave VFEL.

In this paper we compare results of simulation of one-dimensional distributed feedback in conditions of BWT and volume (non-one-dimensional) distributed feedback in VFEL. We chose parameters of one-dimensional geometry corresponding to backward Bragg diffraction. Then we change them by varying transverse components of wave vector  $\mathbf{k}$  and reciprocal lattice vector with the aim to found parameters for more effective generation.

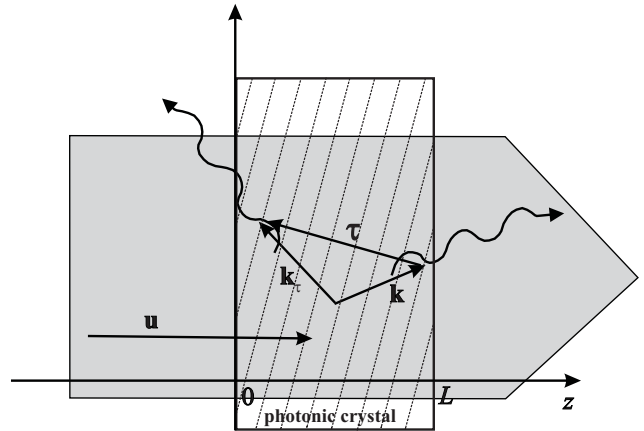


FIG. 2: Common scheme of VFEL.

## 2. VFEL basic equations

Let us consider VFEL with grid resonator in which two-wave geometry of diffraction is realized (see Fig.1). In Fig.2 a model of such two-dimensional system is given. Here an electron beam with electron velocity  $\mathbf{u}$  and electron current density  $j_0$  passes through a photonic crystal (resonator) of the length  $L$ .

Electromagnetic field is described as follows:

$$\mathbf{E}(\mathbf{r}, t) = \mathbf{e}(Ee^{i(\mathbf{k}\mathbf{r}-\omega t)} + E_\tau e^{i(\mathbf{k}_\tau\mathbf{r}-\omega t)})$$

where  $\mathbf{e}$  is vector of polarization.  $E$  and  $E_\tau$  are complex-valued amplitudes of two strong electromagnetic waves with wave vectors  $\mathbf{k}$  and  $\mathbf{k}_\tau = \mathbf{k} + \boldsymbol{\tau}$  excited in the resonator under diffraction conditions. First one is transmitted wave, second one is diffracted wave. Here  $\boldsymbol{\tau}$  is reciprocal lattice vector of photonic crystal.  $\omega$  is frequency.

If simultaneously electrons are under synchronism condition with transmitted wave:  $|\omega - \mathbf{k}\mathbf{u}| \approx 0$ , they emit electromagnetic radiation in directions depending on diffraction conditions.

In [17] the system of equations describing electromagnetic field dynamics in VFEL for two-wave geometry was suggested. In [18] it was considered three-wave case. Electron beam dynamics is simulated via method of averaging over initial phases of electrons [9]. This method is well-known and widely used in simulation of microwave electronic vacuum devices [6].

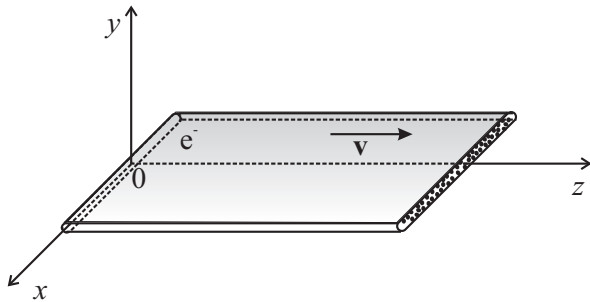


FIG. 3: Annular electron beam.

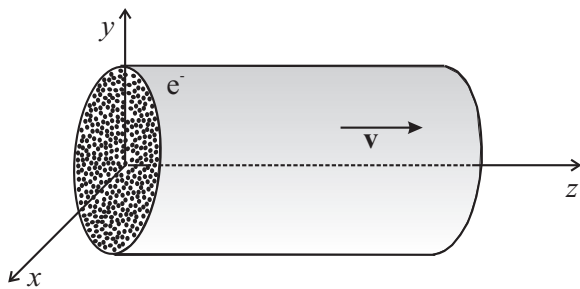


FIG. 4: Ribbon electron beam.

The majority of microwave electronic devices use annular or ribbon electron beams [6] (see Fig.3 and Fig.4). Such beams interact with the slow-wave system or the surface of resonator and should pass over the surface at small distance  $d \leq \frac{\lambda\beta\gamma}{4\pi}$ , where  $\gamma$  is the Lorentz factor of electron beam,  $\beta = u/c$ ,  $c$  is velocity of light. In simulation of such systems method of averaging over initial phases of electrons [9], [6] doesn't take into account transverse coordinates of electron coming in the resonator but only the moment of entrance.

There exist different types of VFEL [4]: with

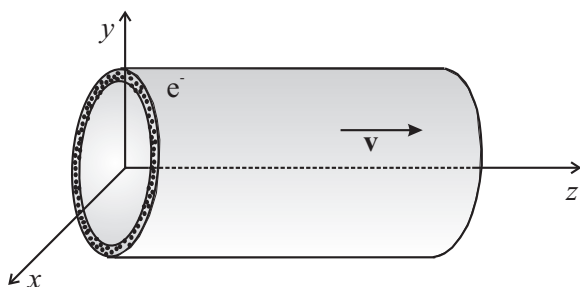


FIG. 5: Wide electron beam.

annular or ribbon electron beams or with wide in cross-section electron beam (see Fig.5). In the last case in [17] it was demonstrated the necessity of consideration both the moment of electron entrance in resonator (as in [9], [6]) and the transverse coordinates of its coming there. But in two first types of electron beam it is not out of place to consider this too.

Let us adduce derivation of expression for beam current density from equations for electromagnetic field and its transition to well-known micro-wave dynamics equations [6].

So, introducing phase of electron coming in resonator at moment of time  $t_0$   $\Theta(t, t_0, \mathbf{r})$  we consider the combination of two initial phases  $\Theta_1$  and  $\Theta_0$ :

$$\Theta(t = t_0, t_0, \mathbf{r}_\perp) = \mathbf{k}_\perp \mathbf{r}_\perp - \omega t_0 = \Theta_1 - \Theta_0 = p \tag{2}$$

where  $\Theta_0, \Theta_1 \in [0, 2\pi]$ ,  $p \in [-2\pi, 2\pi]$ . Averaging over this combination of phases allows to pass from microscopical description of electron beam to the macroscopical one:

$$J = j_0 \int_0^{2\pi} \frac{d\Theta_1}{2\pi} \int_0^{2\pi} \frac{d\Theta_0}{2\pi} e^{-i\Theta(t,z,\Theta_1-\Theta_0)}, \tag{3}$$

Further reduction of (3) can be obtain by decomposition of plane figure into integral sums well-known in mathematical analysis. Let us introduce regular grid with step  $\Delta\vartheta$ :  $N\Delta\vartheta = 2\pi$  when  $N \rightarrow \infty$ . Then

$$\int_0^{2\pi} d\Theta_1 \int_0^{2\pi} d\Theta_0 e^{-i\Theta(t,z,\Theta_1-\Theta_0)} \approx \sum_{k=0}^N \sum_{j=0}^N e^{-i\Theta((j-k)\Delta\vartheta)} \Delta\vartheta^2 \quad (4)$$

$$= \sum_{k=0}^N (e^{-i\Theta(k\Delta\vartheta)} + e^{-i\Theta(-k\Delta\vartheta)}) (N-k) \Delta\vartheta^2 \approx \int_0^{2\pi} (e^{-i\Theta(t,z,p)} + e^{-i\Theta(t,z,-p)}) (2\pi-p) dp.$$

If we neglect the transverse phase  $\Theta_1$  as in [9], [6], the transformation chain (3):

$$\sum_{k=0}^N \sum_{j=0}^N e^{-i\Theta((j-k)\Delta\vartheta)} \Delta\vartheta^2 \quad (5)$$

$$= \sum_{k=0}^N e^{-i\Theta(-k\Delta\vartheta)} N \Delta\vartheta^2 \approx 2\pi \int_0^{2\pi} e^{-i\Theta(t,z,-p)} dp.$$

leads immediately to well-known right-hand side of micro-wave dynamics equations [6].

So, from Maxwell equations in slowly-varying amplitudes approximation the system of equations describing nonlinear stage of VFEL operation of the following form is derived:

$$\frac{\partial E}{\partial t} + \gamma_0 c \frac{\partial E}{\partial z} + 0.5i\omega l E - 0.5i\omega \chi_\tau E_\tau = I,$$

$$\frac{\partial E_\tau}{\partial t} + \gamma_1 c \frac{\partial E_\tau}{\partial z} + 0.5i\omega \chi_{-\tau} E - 0.5i\omega l_1 E = 0,$$

$$I = \frac{j_0 \Phi}{4\pi} \times \int_0^{2\pi} (2\pi-p) \left( e^{-i\Theta(t,z,p)} + e^{-i\Theta(t,z,-p)} \right) dp,$$

$$\frac{\partial^2 \Theta(t,z,p)}{\partial z^2} = \frac{e\Phi}{m\gamma^3 \omega^2} \left( k_z - \frac{\partial \Theta(t,z,p)}{\partial z} \right)^3$$

$$\times \text{Re} \left( E_0(t-z/u, z) e^{i\Theta(t,z,p)} \right),$$

$$\Theta(t, 0, p) = p, \quad \frac{\partial \Theta(t, 0, p)}{\partial z} = k_z - \omega/u.$$

Here  $t > 0$ ,  $z \in [0, L]$ ,  $p \in [-2\pi, 2\pi]$ .  $\gamma_0 = \frac{k_z}{k}$ ,  $\gamma_1 = \frac{k_{\tau z}}{k}$  are distributed feedback cosines.

$l = l_0 + \delta$ ,  $l_{0,1} = (k_{\tau}^2 c^2 - \omega^2 \epsilon_0) / \omega^2$ .  $\epsilon_0 = 1 + \chi_0$ ,  $\chi_0$ ,  $\chi_{\pm\tau}$  are Fourier components of the dielectric susceptibility of resonator.  $\delta$  is detuning from exact synchronism condition.  $\Phi = \sqrt{l_0 + \chi_0 - 1/(\beta\gamma)^2}$ .

Boundary conditions for the system can have different forms including external reflectors [17]. Their simplest form corresponding to Fig.2 is the following:

$$E(t, z=0) = E_0, \quad E_\tau(t, z=L) = 0.$$

### 3. Results of numerical simulation

In this article we examine the influence of non-one-dimensional distributed feedback to dynamics of VFEL generation. We compare two-dimensional Bragg geometry (see Fig.6, dashed lines) with one-dimensional backward geometry. Its wave vectors are shown in solid lines in Fig.6. As initial data we take the following parameters of grid resonator [12]: length  $L = 15$  cm with thread period on axis  $z$  12.5 mm, the generation frequency 10.4 GHz, beam current density  $j_0 = 300$  A/cm<sup>2</sup>.

In Fig. 7 it is shown the time dependence of amplitudes of transmitted wave (lower curve) and diffracted wave (upper curve) at the outlet of resonator in BWT geometry for the value of the detuning from synchronism condition  $\delta = 0$ . One can see that these dependencies are almost periodic (weak chaos).

Everywhere below we will consider the wave amplitudes at the outlet of photonic crystal.

Let us consider dependence of wave ampli-

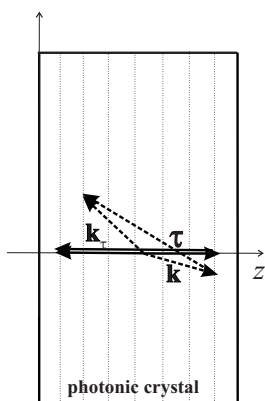


FIG. 6. Scheme of BWT geometry (solid lines) and two-dimensional Bragg geometry (dashed lines).

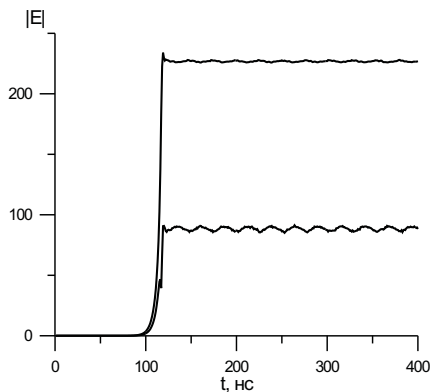


FIG. 7. Time dependence of amplitudes of transmitted wave (lower curve) and diffracted wave (top curve) in one-dimensional backward geometry.

tudes on changes of diffraction geometry parameters  $k_x$  and  $\tau_x$  in the case  $\delta = 0$  (Fig.8) as well corresponding parametric maps of chaotic lasing (Fig.9). We see very smooth dependencies (Fig.8) with small absolute values of amplitudes. Parametric maps (Fig.9) contain only a strip of stationary generation along the generation threshold, periodical and weak chaotic regimes. Two spots of periodicity are on the field of weak chaos for transmitted wave. And one spot of chaos is situated near the origin of coordinates for diffracted wave.

Then let us change a little the value of detuning from synchronism condition  $\delta$ . Such deviation exists always. It is impossible to satisfy

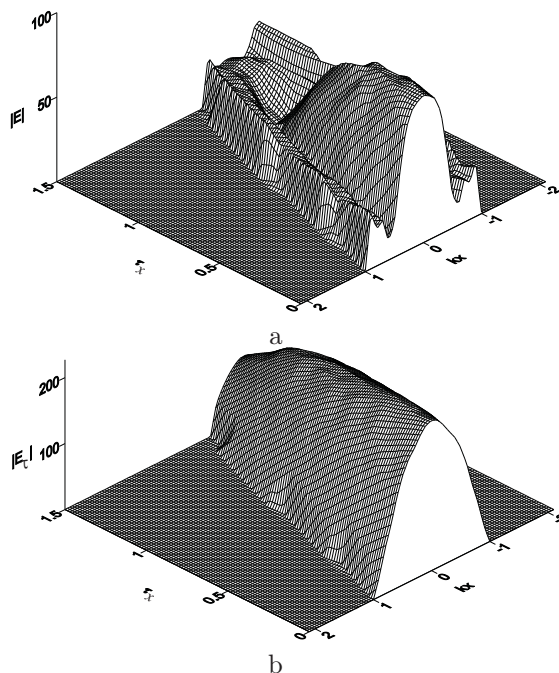


FIG. 8. Amplitudes for transmitted (a) and diffracted (b) waves when changing  $k_x$  and  $\tau_x$ .  $\delta = 0$ .

synchronism condition exactly. The changing of  $\delta$  to positive values gives the same pictures as in Fig.8 and Fig.9. Negative values of  $\delta$  leads to more interesting results given below.

In Fig.11 dependence of wave amplitudes on changes of diffraction geometry parameters  $k_x$  and  $\tau_x$  is shown. We see that for  $\tau_x = 0$  symmetrical pattern of generation when changing  $k_x$  to the right and to the left of zero shifts and transforms with increasing of  $\tau_x$  values till 1.5. There are essentially large absolute values of amplitudes than in previous case (Fig.8). At BWT geometry for  $k_x = 0$  and  $\tau_x = 0$  there are small values of amplitudes in comparison with other points.

In Fig.11 parametric maps of VFEL dynamical regimes are given for two parameters of geometry:  $\tau_x$  and  $k_x$ . On edges of maps the most typical dependencies of electromagnetic field intensities  $|E(t, L)|$  and  $|E_\tau(t, 0)|$  on time (in ns) are presented.

Unlike the previous parametric maps obtained in [20], [22] as well as given in Fig.9, in Fig.11 we have a strip of chaotic self-oscillations

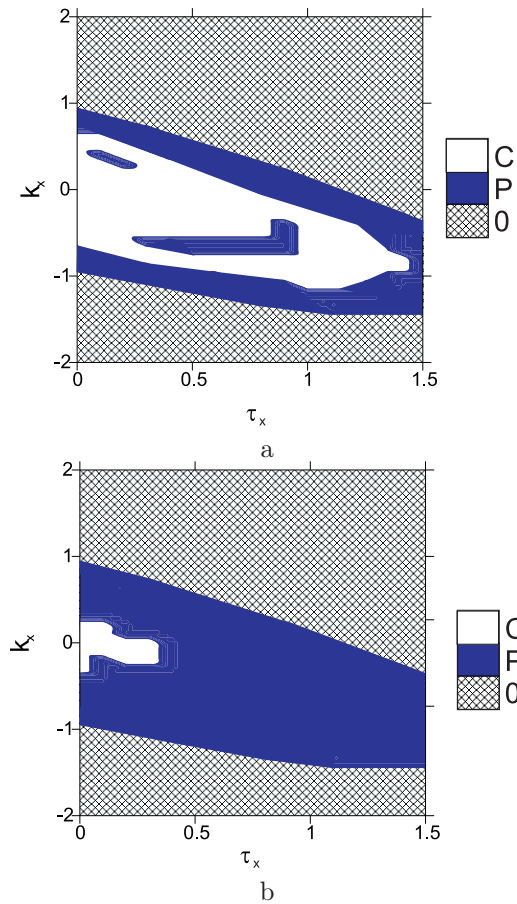


FIG. 9. Parametric maps of chaotic lasing for transmitted (a) and diffracted (b) waves when changing  $\tau_x$  and  $k_x$ .  $\delta = 0$ . 0 depicts domain under generation threshold. P and C correspond to periodic regimes and chaos, respectively.

along the generation threshold, then it changes into the strip of intermittency and the strip of transition between large-scale and small-scale amplitudes in Fig.11. In the center of maps there are overlaps of periodic, quasiperiodic and different chaotic regimes.

It is obvious that all maps for diffracted wave are less variegated, with the smaller number of main frequencies than for transmitted one. This is numerical validation of one important VFEL physical feature consisting in suppression of spurious modes inside the resonator. Due to mechanism of VDFB in conditions of diffraction in resonator not all parasitic frequencies arising in elec-

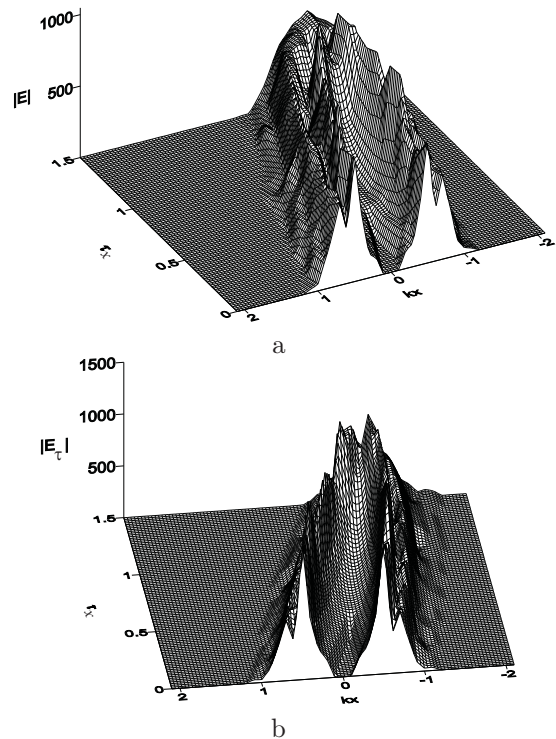


FIG. 10. Dependence of wave amplitudes on changes of diffraction geometry for transmitted (a) and diffracted (b) waves.

tron beam moving through resonator are passed from the electron beam to the transmitted electromagnetic wave and all the more to the diffracted one. This was demonstrated numerically earlier for other cases in [22].

In Fig.12 for data corresponding to Fig.10 transition between dynamical regimes for  $k_x = 0$  and six values of  $\tau_x$  are presented. This series of plots shows mostly chaotic oscillations for transmitted wave (plots 1,a–5,a) and for diffracted wave (4,b), (5,b), as well as periodic and quasi-periodic oscillations (1,b)–(4,b), (6,a), (6,b).

System parameters  $k_x = 0$  and  $\tau_x = 1.5$  gives results under generation threshold.

Now let us change the value of transverse component  $k_x = -0.5$ . In Fig.13 plots for dynamical regimes for seven values of  $\tau_x$  are presented. In this case periodic regimes are dominant. The values of amplitudes for  $k_x = 0$  (Fig.12) and  $k_x = -0.5$  (Fig.13) differ from more than two times till one order.

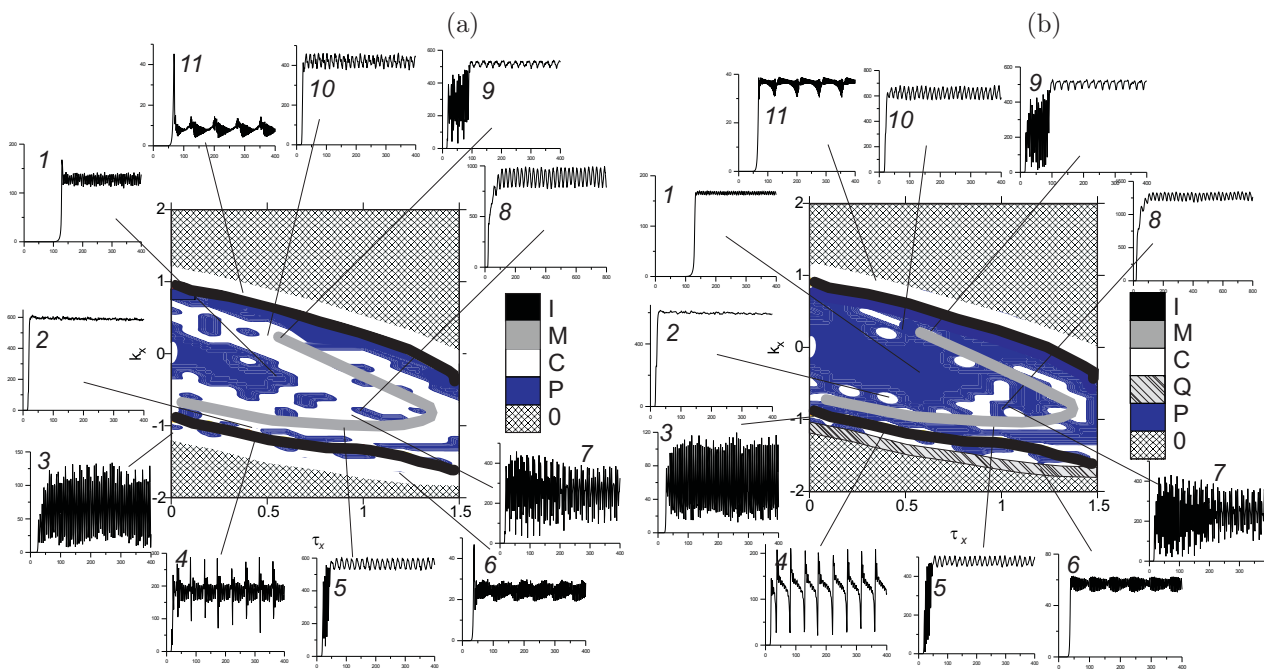


FIG. 11. Parametric maps of chaotic lasing for transmitted (a) and diffracted (b) waves when changing  $\tau_x$  and  $k_x$ . 0 depicts domain under generation threshold. P, Q, C correspond to periodic, quasiperiodic regimes and chaos, respectively. M corresponds to transition between large-scale and small-scale amplitudes. I describes intermittency.

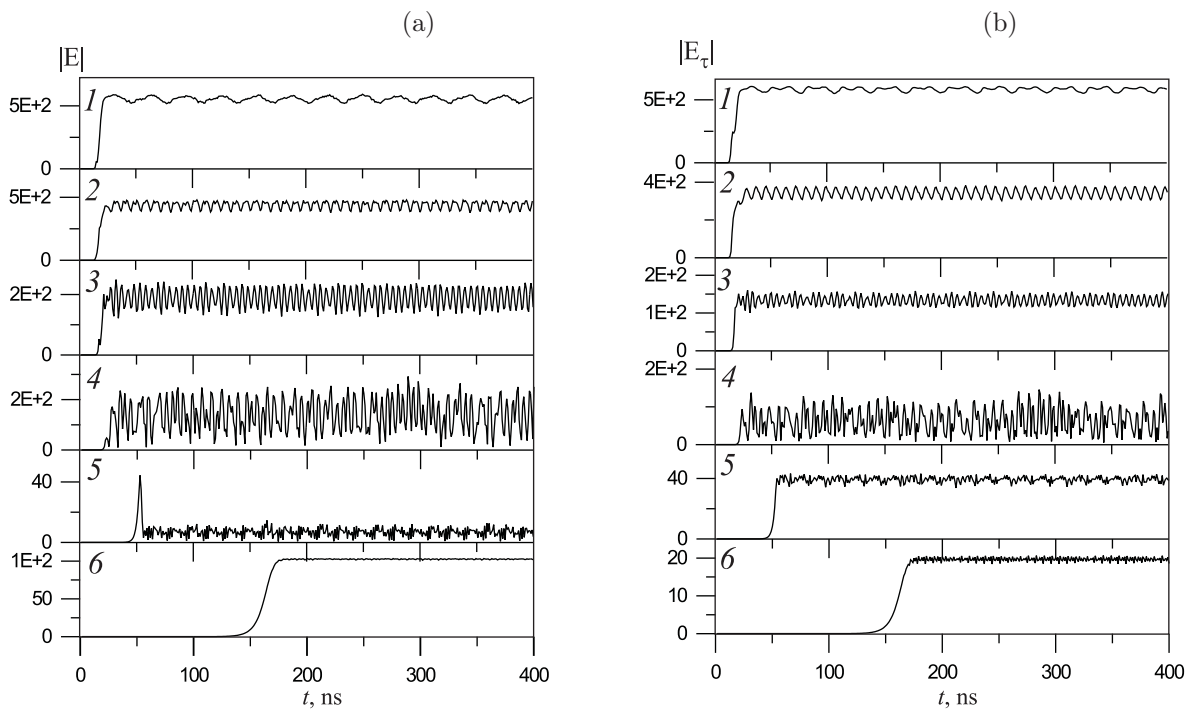


FIG. 12. Transition between dynamical regimes for transmitted (a) and diffracted (b) waves under changing of  $\tau_x$ .  $k_x = 0$ . (1):  $\tau_x = 0.9$ ; (2):  $\tau_x = 1.0$ ; (3):  $\tau_x = 1.1$ ; (4):  $\tau_x = 1.2$ ; (5):  $\tau_x = 1.3$ ; (6):  $\tau_x = 1.4$ .

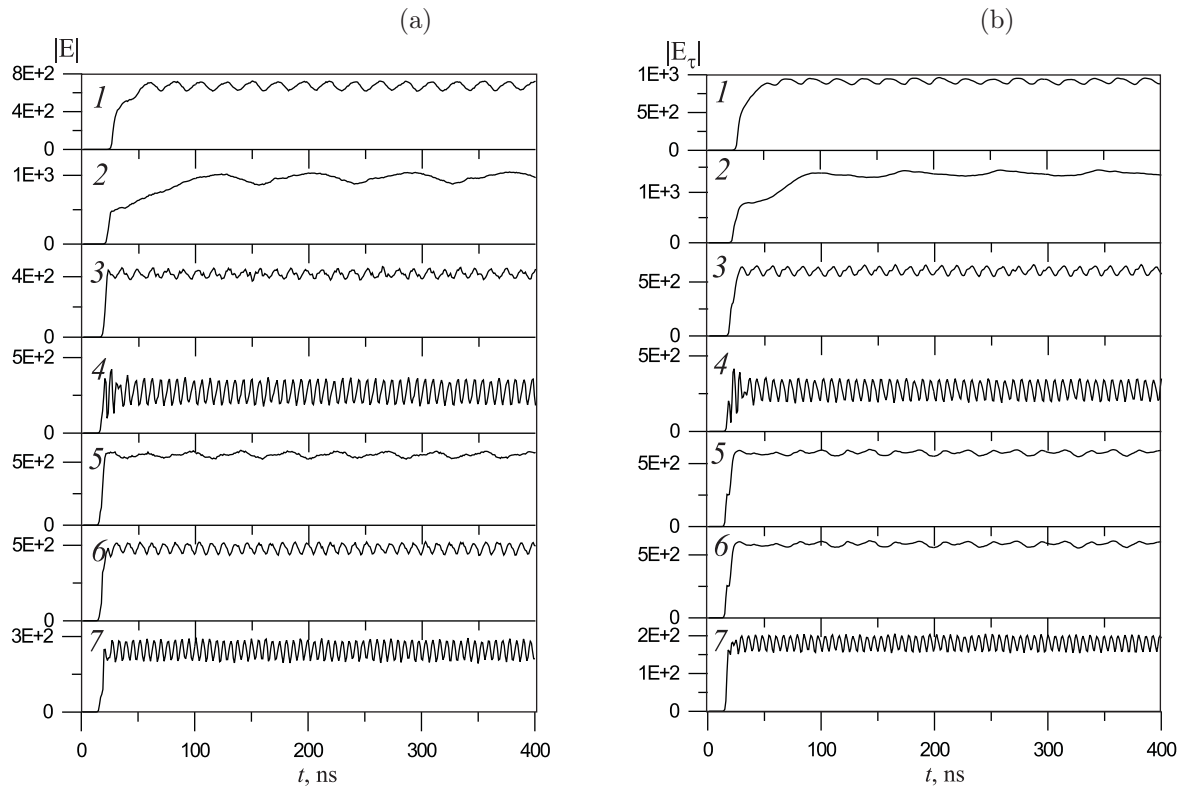


FIG. 13. Transition between dynamical regimes for transmitted (a) and diffracted (b) waves under changing of  $\tau_x$ .  $k_x = -0.5$ . (1):  $\tau_x = 0.9$ ; (2):  $\tau_x = 1.0$ ; (3):  $\tau_x = 1.1$ ; (4):  $\tau_x = 1.2$ ; (5):  $\tau_x = 1.3$ ; (6):  $\tau_x = 1.4$ ; (7):  $\tau_x = 1.5$ .

Thus, we can conclude that variation from one-dimensional to non-one-dimensional geometry leads to changing in the type of dynamical solution. So, the choice of VFEL geometry can implement periodic dynamics rather chaotic regime.

#### 4. Conclusion

As VFEL physical principles differ from ones of other vacuum electronic devices VFEL is an interesting object of investigation with specific characters, suitable for generation of powerful electromagnetic radiation in different wavelength ranges. In VFEL simulation different sides of VFEL nonlinear dynamics were investigated with the object of its experimental investigation.

It was demonstrated that multi-dimensional volume distributed feedback in VFEL can give more large values on amplitudes than one-dimensional distributed feedback. The possible way of chaos control in VFEL can be realized via changing of VDFB geometry.

#### Acknowledgments

Author thanks Prof. V. G. Baryshevsky for permanent interest to the work.

## References

- [1] V.G. Baryshevsky, I.D. Feranchuk. Parametric beam instability of relativistic charged particles in a crystal. *Phys. Lett. A*. **102**, 141-144 (1984).
- [2] V.G. Baryshevsky, K.G. Batrakov, I.Ya. Dubovskaya. Parametric (quasi-Cherenkov) X-ray free electron laser. *J. Phys. D*. **24**, 1250-1257 (1991).
- [3] V.G. Baryshevsky, I.D. Feranchuk, A.P. Ulyanov. *Parametric X-ray radiation in crystals: theory, experiment and applications*. Series: Springer Tracts in Modern Physics. (Springer, 2005).
- [4] V.G. Baryshevsky. High Power Microwave and Optical Volume Free Electron Lasers (VFELs). arXiv:1211.4769v1 [physics.optics]. 35 p.
- [5] V.G. Baryshevsky. *High-energy nuclear optics of polarized particles* (World Press, 2012).
- [6] D.I. Trubetskov, A.E. Hramov. *Lectures on microwave electronics for physicists* (Fizmatlit, Moscow, 2003)(in Russian).
- [7] Erohin N.S., Kuzelev N.V., Moiseev S.S. et al. *Non-equilibrium and equilibrium processes in plasma radiophysics* (Nauka, Moscow, 1982).
- [8] T. Marshall. *Free-Electron Laser* (Macmillan Pub. Company, New York, 1985).
- [9] L.A. Vainshtein, V.A. Solncev. *Lectures on microwave electronics* (Soviet Radio, Moscow, 1973)(in Russian).
- [10] V.G. Baryshevsky, A.A. Gurinovich. Spontaneous and induced parametric and Smith-Purcell radiation from electrons moving in a photonic crystal built from the metallic threads. *Nucl. Instr. Meth. Phys. Res.* **B252**, 92-101 (2006).
- [11] V.G. Baryshevsky, K.G. Batrakov, A.A. Gurinovich et al. First lasing of a volume FEL (VFEL) at a length range  $\lambda \sim 4-6$  mm. *Nucl. Instr. Meth. Phys. Res.* **bf A483**, 21-23 (2002).
- [12] V.G. Baryshevsky, N.A. Belous, A.A. Gurinovich et al. Experimental studies of Volume FELs with a photonic crystal. *Proc. 35th Int. Conf. on Infrared, Millimeter, and Terahertz Waves. IR-MMWTHz*. 2 p. (2010).
- [13] E. Yablonovich, T.J. Gmitter. Photonic band structure: the face-centered-cubic case. *Phys. Rev. Lett.* **63**, 1950-1953 (1989).
- [14] E. Yablonovich. Photonic crystals: what's in a name. *Light Touch Column from the March 2007. Issue of Optics & Photonics News*. 2 p.(2007).
- [15] C. Luo, M. Ibanescu, S. Johnson, J. Joannopoulos. Cherenkov radiation in photonic crystals. *Science*. **299**, 368-371 (2003).
- [16] P.M.J. van der Slot, T. Denis, J.H.H. Lee et al. Photonic Free-Electron Lasers. *IEEE Photonic Journal*. **4**, 570-573 (2012).
- [17] K.G. Batrakov, S.N. Sytova. Modelling of Volume Free Electron Lasers. *Computational Mathematics and Mathematical Physics*. **45**, 666-676 (2005).
- [18] K.G. Batrakov, S.N. Sytova. Dynamics of electron beam instabilities under conditions of multiwave distributed feedback. *Int. J. Nonlinear Phenomena in Complex Systems*. **8**, 359-365 (2005).
- [19] S.N. Sytova. Volume Free Electron Laser (VFEL) as a dynamical system. *Int. J. Nonlinear Phenomena in Complex Systems*. **10**, 297-302 (2007).
- [20] S.N. Sytova. Numerical Analysis of Lasing Dynamics in Volume Free Electron Laser. *Mathematical Modelling and Analysis*. **13**, 263-274 (2008).
- [21] S.N. Sytova. Some aspects of chaotic lasing in volume free electron lasers. *Nonlinear Phenomena in Complex Systems*. **12**, 37-45 (2009).
- [22] S.N. Sytova. Chaos in Volume Free Electron Lasers (VFEL). *Applied Nonlinear Dynamics*. **19**, 93-111 (2011).